Cell Transplantation, Vol. 24, pp. 2513–2525, 2015

0963-6897/15 $90.00 + .00
DOI: http://dx.doi.org/10.3727/096368915X686779
E-ISSN 1555-3892
www.cognizantcommunication.com

3D-Printed Drug/Cell Carrier Enabling Effective Release of Cyclosporin A for Xenogeneic Cell-Based Therapy

Tae-Ha Song,*†[1] Jinah Jang,*[1] Yeong-Jin Choi,‡ Jin-Hyung Shim,§ and Dong-Woo Cho*

*Department of Mechanical Engineering, Pohang University of Science and Technology (POSTECH), Hyoja-dong, Nam-gu, Pohang, Kyungbuk, Korea
†Medical Device Development Center, Daegu-Gyeongbuk Medical Innovation Foundation (DGMIF), Dong-gu, Daegu, Korea
‡Division of Integrative Biosciences and Biotechnology, Pohang University of Science and Technology (POSTECH), Hyoja-dong, Nam-gu, Pohang, Kyungbuk, Korea
§Department of Mechanical Engineering, Korea Polytechnic University, Siheungsi, Gyeonggi-do, Korea

Systemic administration of the immunosuppressive drug cyclosporin A (CsA) is frequently associated with a number of side effects; therefore, sometimes it cannot be applied in sufficient dosage after allogeneic or xenogeneic cell transplantation. Local delivery is a possible solution to this problem. We used 3D printing to develop a CsA-loaded 3D drug carrier for the purpose of local and sustained delivery of CsA. The carrier is a hybrid of CsA-poly(lactic-*co*-glycolic acid) (PLGA) microsphere-loaded hydrogel and a polymeric framework so that external force can be endured under physiological conditions. The expression of cytokines, which are secreted by spleen cells activated by Con A, and which are related to immune rejection, was significantly decreased in vitro by the released CsA from the drug carrier. Drug carriers seeded with xenogeneic cells (human lung fibroblast) were subcutaneously implanted into the BALB/c mouse. As a result, T-cell-mediated rejection was also significantly suppressed for 4 weeks. These results show that the developed 3D drug carrier can be used as an effective xenogeneic cell delivery system with controllable immunosuppressive drugs for cell-based therapy.

Key words: 3D printing; Drug delivery system; Cyclosporin A; Cell-based therapy; T-cell-mediated rejection

INTRODUCTION

Cell-based therapy (CBT) has been developed as a promising approach for treatment of diseases such as muscular dystrophy, degenerative disc disease, or myocardial infarction (11,12,45). However, CBT requires use of allogeneic or xenogeneic cells, which stimulate an immune rejection response (11,12,45,48,50), so immunosuppressive drugs must be administered to prevent acute transplant rejection after cell transplantations (9,26). Calcineurin inhibitors such as cyclosporin A (CsA) or tacrolimus (FK506) are the most widely used immunosuppressive drugs (6,20,43). They deactivate a nuclear factor of activated T-cell (NFATc) protein so that immune rejection-related cytokines like interleukin-2 (IL-2), IL-17, and interferon-γ (IFN-γ) cannot be encoded in the early phase of T-cell activation (28). The introduction of CsA improves the success rate of various transplantations (3,14,25), but systemic administration of CsA requires a high dose of drug, which causes severe side effects such as nephrotoxicity, hypertension, dyslipidemia, gingivitis, and hirsutism (19). To avoid these problems, local CsA delivery of a relevant dose of drugs can be a promising solution.

Many trials have attempted CsA delivery using delivery systems based on microspheres or hydrogels, but most reports were limited to systemic delivery of CsA (44) and mostly considered ophthalmic (17,46) or dermatological (21) applications. These delivery systems have some critical problems. Microsphere-based drug delivery systems can cause embolisms or further organ damage due to emigration of the microspheres from the injection site (37). Furthermore, microspheres are susceptible to phagocytosis by macrophages (34). Hydrogel-based delivery systems can result in relatively rapid drug release over intervals of a few hours to a few days; this speed may be undesirable. Moreover, the weak mechanical properties of hydrogel preclude its application to sites that have highly demanding load-bearing capacity. Low mechanical properties usually cause premature dissolution during material injection. Moreover, the intermolecular dispersion phenomenon inhibits releasing the encapsulated

Received July 8, 2014; final acceptance January 12, 2015. Online prepub date: January 20, 2015.
[1]These authors provided equal contribution to this work.
Address correspondence to Dong-Woo Cho, Department of Mechanical Engineering, Pohang University of Science and Technology (POSTECH), San 31, Hyoja-dong, Nam-gu, Pohang, Kyungbuk 790-784, Korea. Tel: +82 54 279 2171; Fax: +82 54 279 5419; E-mail: dwcho@postech.ac.kr

drugs, which are located within the hydrophilic releasing system. (8,18).

Several studies have considered local (19,32) or sustained (33) delivery of CsA, but none have considered local and sustained release simultaneously to prevent immune rejection of transplanted tissues. The objectives of this study are to show the feasibility of using a subcutaneous 3D-printed drug delivery system to achieve local and sustained release and investigate local immunosuppressive effects of CsA after xenogeneic cell transplantation.

MATERIALS AND METHODS

Animals

Seven- to 10-week-old C57BL/6 male mice and 6-week-old BALB/c male mice were purchased from Orient Bio (Seoul, Korea). All animal protocols were approved by Institutional Animal Care and Use Committee of POSTECH.

Materials

Cyclosporin A (CsA) (BML-A195-0500, MW 1202.6, purity≥98%) was purchased from Enzo Biochem (New York, NY, USA). Poly(lactic-*co*-glycolic acid) (PLGA) (430471-5G, MW 50,000–75,000), alginic acid sodium salt (alginate; A0682-100G, low viscosity), concanavalin A (ConA) (L7647-100MG), HEPES buffer, eosin, and poly(vinyl alcohol) (PVA) (363073-500G, MW 31,000–50,000) were purchased from Sigma-Aldrich (St. Louis, MO, USA). Polycaprolactone (PCL) (19561-500G, MW 43,000–50,000) was purchased from Polysciences (Warrington, PA). Hematoxylin was purchased from Dako (Carpinteria, CA, USA). RPMI-1640 and DMEM high-glucose were purchased from Hyclone (Logan, UT, USA). Fetal bovine serum (FBS) and antibiotics (penicillin–streptomycin) were purchased from Gibco (Grand Island, NY, USA). 2-Mercaptoethanol was purchased from Biosesang (Seongnam, Korea). Optimal cutting temperature (OCT) compound was purchased from Tissue-Tek (Miles Laboratories, Elkhart, IN, USA). Dichloromethane (DCM) [M0821, assay (GC)≥98%] was purchased from Samchun Chemicals (Seoul, Korea). Calcium chloride ($CaCl_2$) (07057-00) was purchased from Kanto Chemical (Tokyo, Japan). Tween 80 (T1004) was purchased from USB (Cleveland, OH, USA).

Fabrication of CsA-Loaded 3D Drug Carriers

Preparation of the Mixture of CsA-Loaded PLGA Microspheres and Alginate Hydrogel. A hydrogel-based drug delivery system is usually restricted to burst release, and a hydrophobic drug cannot be easily loaded directly into the hydrophilic carrier. To encapsulate hydrophobic drugs into the hydrogel stably and homogeneously, we prepared hydrophobic drug-loaded polymeric microspheres (Fig. 1). The mixture of drug-loaded microsphere and hydrogel enables sustained drug release (22,42). In this study, CsA, which is hydrophobic, was loaded into PLGA microspheres, which were mixed with alginate hydrogel.

The CsA-loaded PLGA microspheres were prepared using the oil-in-water solvent evaporation technique (7) (Fig. 1a). Briefly, an organic phase was prepared by dissolving 120 mg of PLGA and 12 mg of CsA in 0.9 ml of DCM. An aqueous phase was prepared by dissolving 180 mg of PVA in 18 ml of deionized (DI) water. A mixture of the organic and aqueous phase was emulsified using a sonicator (Sonic Dismembrator Model 100; Fisher Scientific, Indiana, PA, USA) for fabricating microspheres (Fig. 1b). The emulsion was formed by sonication at 6-W output power for 90 s. The prepared emulsion was mixed with 50 ml of 0.1 wt% PVA solution and gently stirred for >4 h to evaporate organic solvents. Then the emulsions were centrifuged and washed three times to remove remaining organic solvents. The microspheres were deep frozen at −70°C and dried in a −90°C freeze dryer (Operon, Gimpo, Korea) for 1 day and stored at −20°C. Finally, the prepared CsA-loaded microspheres were loaded into the 8 wt% alginate hydrogel.

Fabrication of CsA-Loaded 3D Drug Carriers. We used our lab-built biomedical 3D printer (38,41) to fabricate a CsA-loaded 3D drug carrier, which is composed of two components: 8 wt% alginate hydrogel loaded with CsA-PLGA microspheres (CsA-Algi gel) and a blended PCL/PLGA synthetic polymer (PCL/PLGA structure) for improving the load-bearing capacity of the whole structure.

PCL and PLGA were mixed thoroughly at a 1:1 ratio (w/w) at 160°C. The blended PCL/PLGA was loaded in a syringe and melted at 125°C, then dispensed at 500 kPa using a pneumatic pressure-regulated dispenser to print three pairs of parallel lines of the PCL/PLGA structure, with pairs joined at alternating ends (Fig. 1c). CsA-Algi gel was dispensed between the lines in each pair using a plunger-based low-dosage dispensing system (Fig. 1d). The printing and dispensing processes were repeated three times to form a layered structure with the lines in each layer oriented right at angles to those in the layer below it (Fig. 1e).

Characterization of CsA-Loaded PLGA Microspheres

Size Distribution of CsA-Loaded PLGA Microspheres. The size (Z-Ave) of the CsA-loaded PLGA microspheres was measured by using dynamic light scattering (Zetasizer, Malvern, UK). The CsA-loaded PLGA microspheres were suspended in an aqueous solution and mixed using a vortexer (Fisher Scientific) before analysis.

Evaluation of Drug Content and Encapsulation Efficiency. The amount of CsA encapsulated in PLGA microspheres was quantified by high-performance liquid chromatography (HPLC) (Waters Alliance 2695). CsA-loaded microspheres were dissolved in acetonitrile

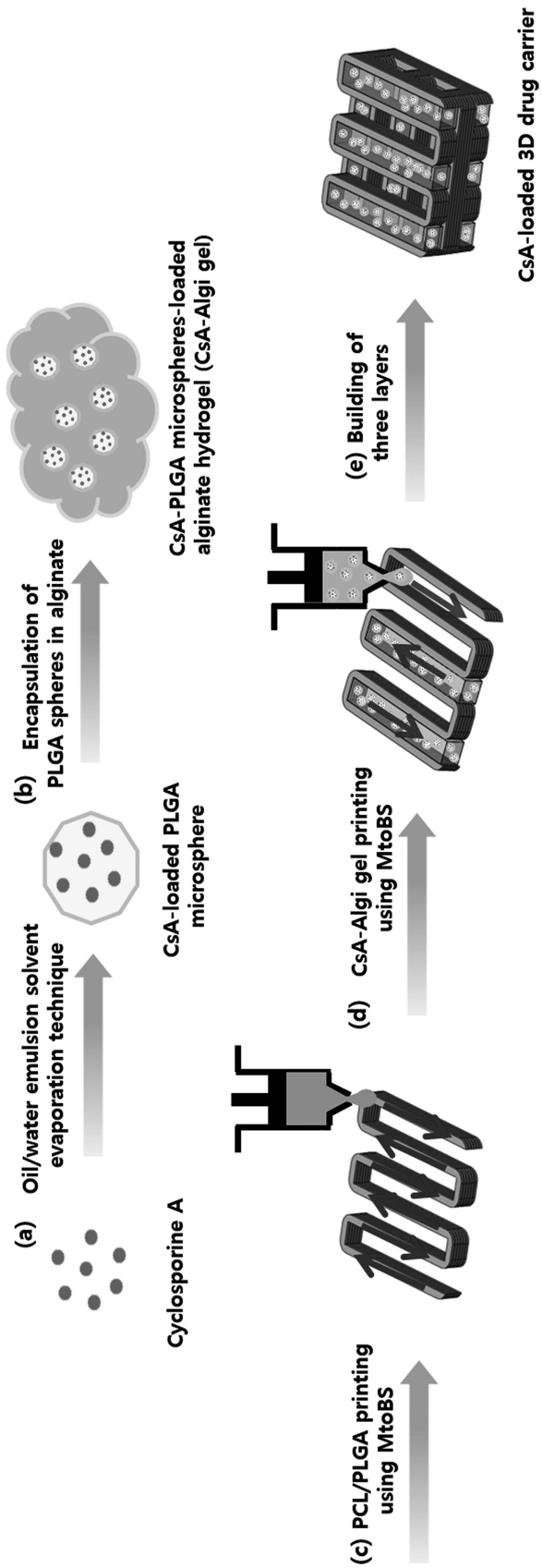

Figure 1. Schematic diagram of the preparation of CsA-loaded 3D drug carriers. (a) Preparation of CsA-loaded PLGA microspheres using the O/W emulsion solvent evaporation technique. (b) Preparation of CsA-Algi gel thorough mixing CsA-loaded microspheres with 8 wt% alginate hydrogel. (c) Printing of blended PCL/PLGA and (d) printing of CsA-Algi gel using a lab-built biomedical 3D printer. (e) Building three layers.

(Burdick & Jackson, Muskegon, MI, USA) and adequately diluted before injection into the HPLC system. Separation was achieved on an XBridge C18 column (4.6×250 mm) (Waters, Milford, MA, USA). The elution was isocratic at 1.0 ml/min with a mobile phase that consisted of a 4:1 (v/v) mixture of acetonitrile and distilled water. The injection volume was 50 µl, and detection was monitored for absorbance at 210 nm.

The CsA drug content was calculated as

$$\text{CsA content (\%)} = \frac{W_{CsA}}{W_{MS}} \times 100\% \quad (1)$$

where W_{CsA} represents the weight of quantified CsA, and W_{MS} represents the weight of CsA-loaded microspheres.

The encapsulation efficiency was calculated as

$$\text{CsA encapsulation efficiency (\%)} = \frac{CsA_{sphere}}{CsA_{total}} \times 100\% \quad (2)$$

where CsA_{sphere} represents the weight of quantified CsA, and CsA_{total} represents the weight of CsA initially added.

Morphological Characterization of CsA-Loaded PLGA Microspheres and 3D Drug Carriers

The morphological analysis of the CsA-loaded microspheres and 3D drug carrier was performed using a scanning electron microscope (SEM) (Hitachi SU-6600, Tokyo, Japan) at an accelerating voltage of 15 kV. Before SEM imaging, samples were deep frozen at −70°C, dried in a −90°C freeze dryer for 1 day, and coated with platinum (Hitachi).

In Vitro Release Profile Test

A cumulative release profile of CsA from CsA-Algi gel was measured using a dialysis method. A total of 10.868 µg of CsA was loaded into PLGA microspheres, which were then mixed with alginate solution at a concentration of 10 wt%, then cross-linked using $CaCl_2$ (Junsei, Tokyo, Japan).

The prepared gel was put inside a cellulose dialysis bag (MW cutoff 3500; Thermo Fischer Scientific, Rockford, IL, USA) with 3 ml of 0.1 M phosphate buffer (pH 7.4) containing 0.01% (w/v) Tween 80. This method avoids the loss of microspheres during the experiment. The dialysis bag with the gel was suspended in the phosphate buffer (16), then incubated at 37°C. At predetermined intervals, 1 ml of suspension was collected, and the same amount of fresh medium was added. The drug release was quantified using HPLC.

Cell Culture

Spleen cells were isolated from C57BL/6 male mice at the age of 7–10 weeks and cultivated in a RPMI-1640 medium supplemented with 10% FBS, 1% antibiotics (penicillin–streptomycin), 10 mM HEPES buffer, and 5×10^{-5} M 2-mercaptoethanol (referred to as a spleen cell culture medium). The cells (1×10^6 cells/well) were cultured in 200 µl of culture medium in 96-well tissue culture plates (Corning, Corning, NY, USA) stimulated with 2 µg/ml of ConA for 3 days (referred to as ConA-activated spleen cells). A human lung fibroblast (HLF, sex unknown) cell line was purchased from Lonza (Basel, Switzerland) and cultured in a DMEM high-glucose medium supplemented with 10% FBS and 1% antibiotics (referred to as a HLF culture medium). All the cells were incubated at 37°C in 100-mm tissue culture plates (BD Biosciences, San Jose, CA, USA), in 5% CO_2 and 95% air.

Cycotoxicity Test of the Fabricated CsA-Loaded 3D Drug Carriers

To verify the cytotoxicity of CsA-loaded 3D drug carriers, HLFs were seeded onto the CsA-loaded 3D drug carrier at a concentration of 5×10^4 cells/drug carrier and cultured for 7 days. A cell counting kit (Cell Counting Kit-8; Dojindo, Kumamoto, Japan) was used to evaluate cell numbers at days 1, 4, and 7.

Enzyme-Linked Immunosorbent Assay for Investigating CsA-Loaded 3D Drug Carriers

ConA-activated spleen cells were used to assess the CsA-loaded 3D drug carriers in vitro. The cells were loaded in a 96-well plate at a concentration of 1×10^6 cells/well and used for all the following assessments

First, a CsA dose-screening test was conducted to find the appropriate concentration of the drug. Concentrations of 1, 10, 100, and 200 µg/ml were selected based on several reports (4,19,27) and applied to the cell-seeded well plate. The cells were cultured for 24 h, and the cells with cell culture media were harvested for further assay.

The immunosuppressive effect of CsA-loaded 3D drug carriers was investigated. In this study, 200 µg/ml of CsA was selected as representative concentration of 3D drug carriers according to the drug dose screening test. 3D drug carriers without CsA were used as a negative control, and ConA-activated spleen cells without CsA treatment was used as a positive control. All the groups were cultured for 24 h and harvested.

The secreted cytokines were quantified using enzyme-linked immunosorbent assay (ELISA) using the supernatant of harvested samples. IL-2, IL-17, and IFN-γ were selected as representative immunomodulatory cytokines, and ELISA was conducted following the manufacturer's instructions (BioLegend, San Diego, CA, USA).

In Vivo Assessments of CsA-Loaded 3D Drug Carriers

To investigate the immunosuppressive function, we implanted CsA-loaded 3D drug carriers with HLF into the

dorsal subcutaneous space of each of five male BALB/c mice. HLFs were seeded onto the CsA-loaded 3D drug carriers [(+)HLF (+)CsA] at 5×10^4 cells/carrier, and the cell-seeded 3D drug carrier without CsA, [(+)HLF (−) CsA] and the 3D drug carrier without CsA [control, (−) HLF (−)CsA] were used as controls. (+)HLF (+)CsA and (+)HLF (−)CsA groups were stabilized for 24 h before implantation. Animal experiments were performed according to the protocol approved by the Animal Care and Use Committee of the Pohang University of Science and Technology, South Korea (2013-0030). The mice were sacrificed, and all 3D drug carriers were retrieved 1, 3, or 4 weeks after implantation and fixed in formalin (Daejung, Gyeonggi, Korea). Samples were embedded in paraffin (two samples/group) and in OCT compound (three samples/group) for histological analysis. Paraffin-embedded samples were sectioned transversely using a microtome for hematoxylin and eosin (H&E) staining. Samples embedded in OCT compound were sliced using a cryotome (Leica, Bensheim, Germany) for immunofluorescence staining. All sections were 5 μm thick.

Infiltration of mononuclear cells such as macrophages and lymphocytes is an important indicator of transplant rejection. Therefore, tissue sections were stained with H&E to evaluate the infiltration of mononuclear cells by xenogeneic cell transplants. At least three SEM images were randomly selected for each group, and the number of mononuclear cell infiltrations was counted manually. Immune rejection responses were evaluated by immunofluorescence staining of the $CD4^+$ and $CD8^+$ T cells. $CD4^+$ antibodies (1:30, α-CD4-biotin; Life Technologies, Paisley, UK) were applied for 15 min, then secondary antibody (1:100, streptavidin-Alexa 594; Molecular Probes, Eugene, OR, USA) was applied for 2 h. $CD8^+$ antibody (1:200, Alexa488-conjugated-α-CD8α; Life Technologies) was applied for 15 min.

All slides were mounted with DAPI (GBI Labs, Mukilteo, WA, USA) solution and were examined under a light microscope (Nikon Eclipse E600; Nikon Instruments, Melville, NY, USA) and confocal laser microscope (Olympus, Tokyo, Japan).

Statistical Analysis

All data are expressed as mean ± standard deviation. All statistical analyses were performed using SigmaPlot software (ver. 10.0; Systat Software Inc., San Jose, CA, USA). Statistical significance was determined using two-tailed Student's *t*-test and one-way analysis of variance (ANOVA), followed by Tukey's test. Differences were considered to be statistically significant at $p < 0.05$.

RESULTS

Characterization of CsA-Loaded 3D Drug Carriers

Characterization of CsA-Loaded PLGA Microspheres. The CsA content of prepared microspheres was 8.65%, and the measured CsA encapsulation efficiency was ~50%.

The surface morphology of microspheres was examined by analysis of SEM images (Fig. 2a). CsA-loaded PLGA microspheres showed rougher surfaces than PLGA microspheres without CsA. The measured average diameter of microspheres was 1.843 μm, and the data (Fig. 2b) were normally distributed.

Morphological Analysis of 3D Drug Carriers. The fabricated 3D drug carrier was $4.2 \times 4.2 \times 1.8$ mm with a pore size of 600 μm and a line width of 200 μm.

We printed the hydrogel selectively in between the lines of the 3D drug carrier so that the carrier maintains pore interconnectivity. The hydrogel was successfully dispensed in alternate spaces between alternate pairs of parallel lines of the PCL/PLGA structure (Fig. 3).

Cell Cytotoxicity of CsA-Loaded 3D Drug Carriers. The CsA-loaded 3D drug carriers (DC-CsA) caused no cytotoxicity. The CsA-loaded 3D drug carrier group showed similar initial cell attachment to the 3D drug carrier without CsA (DC) group, and all groups had similar proliferation rates for 7 days (Fig. 4).

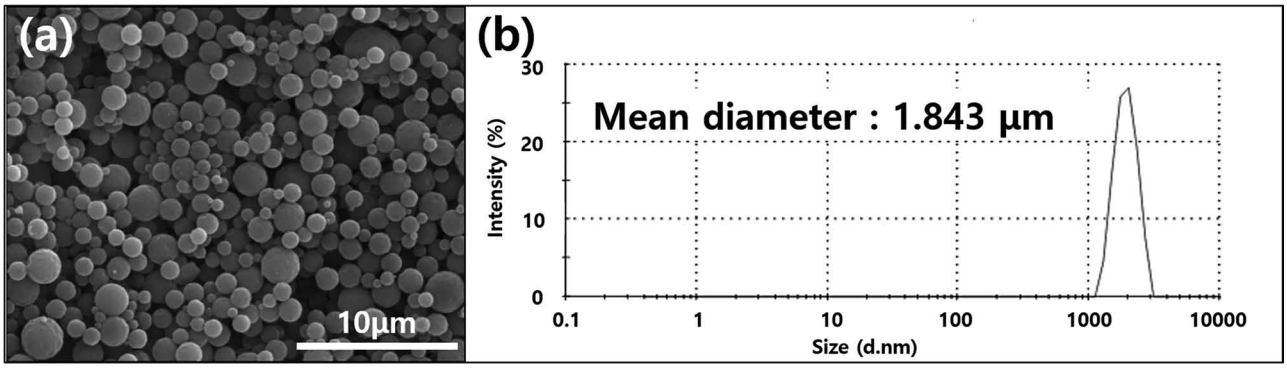

Figure 2. Analysis of the prepared CsA-loaded PLGA microspheres. (a) SEM analysis of the prepared CsA-loaded PLGA microspheres. (b) Intensity particle size distributions of CsA-loaded PLGA microspheres (Zetasizer, mean diameter: 1.843 μm).

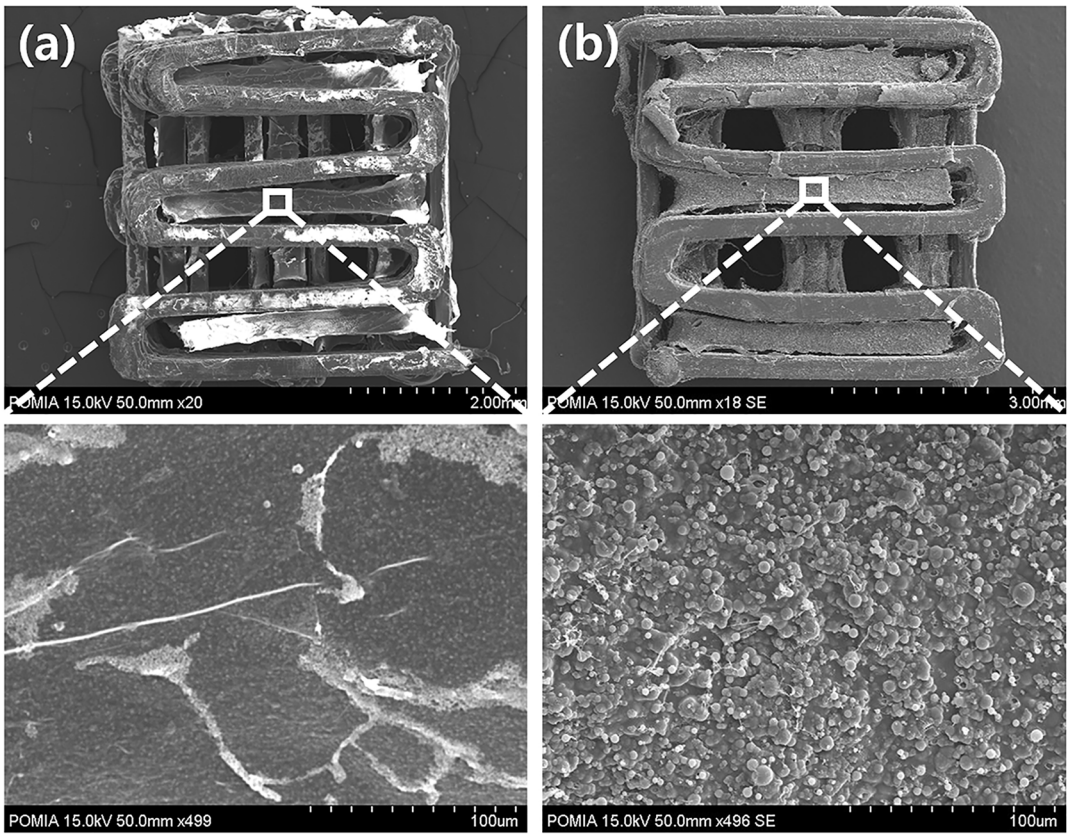

Figure 3. SEM images of 3D drug carrier. (a) 3D drug carrier without CsA (PCL/PLGA + 8 wt% alginate hydrogel), (b) CsA-loaded 3D drug carrier (PCL/PLGA + 8 wt% alginate hydrogel + CsA-loaded PLGA microsphere).

In Vitro Drug Release Profile Test

A cumulative release profile of CsA from the CsA-Algi gel showed an initial burst release followed by a sustained release of CsA (Fig. 5) (1). After burst release on day 1, CsA-Algi gel released drugs sustainedly for 4 weeks, and almost 75% of CsA was released from the CsA-Algi gel by day 28.

Determination of Effective Drug Concentration

Cytokine expression decreased significantly as CsA concentration increased, and the 200 μg/ml dosage suppressed IL-2, IL-17, and IFN-γ secretion effectively (Fig. 6). Based on these results, 200 μg/ml CsA was determined as an effective concentration and was used when fabricating the CsA-loaded 3D drug carrier.

Evaluation of Immunomodulatory Effect of CsA-Loaded 3D Drug Carriers

Immunomodulatory Effect of CsA-Loaded 3D Drug Carriers In Vitro. The DC-CsA group significantly inhibited secretion of IL-2, IL-17, and IFN-γ cytokines; the DC group did not (Fig. 7).

Immunomodulatory Effect of CsA-Loaded 3D Drug Carriers In Vivo. In this experiment, we seeded HLFs on the fabricated 3D drug carriers and subcutaneously implanted them into a BALB/c mouse to confirm their immuno modulatory effects, as well as their prospects as xenogeneic cell carriers (Fig. 8a). Infiltration by mononuclear cells was observed by H&E staining. To verify T-cell-mediated rejection, numbers of $CD4^+$ and $CD8^+$ T cells were quantified using immunofluorescence staining. Overall, the level of the mononuclear cell infiltration decreased over time in all groups and was highest in the (+)HLF (−)CsA group for the entire month (Fig. 8b, c). After 1 week, the level of mononuclear cell infiltration of (+)HLF (+)CsA group was slightly higher than that of the control group, but the number of cells eventually decreased with time and was similar to that of the control group after 3 and 4 weeks. To verify the immune rejection phenomena of xenogeneic cells, we conducted immunofluorescence staining of the $CD4^+$ and $CD8^+$ T cells, which mainly indicate helper T cells and cytotoxic T cells, respectively. The overall transplant rejection response decreased from 1 to 4 weeks. T-cell-mediated immune response did not appear in the control

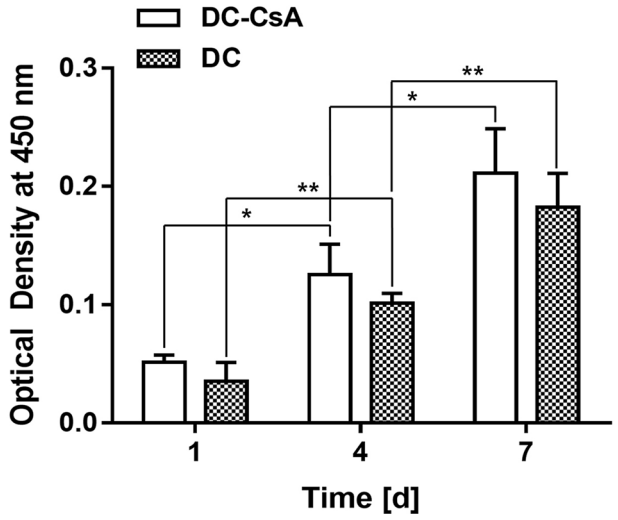

Figure 4. CCK assay for the attachment and proliferation of HLF on fabricated 3D drug carriers with and without CsA (DC, 3D drug carriers without CsA; DC-CsA, CsA-loaded 3D drug carriers). $*p<0.05$, $**p<0.005$.

group, whereas $CD4^+$ and $CD8^+$ T cells were significantly more numerous in the (+)HLF (−)CsA group than in the (+)HLF (+)CsA group during all 4 weeks (Fig. 9). All the implanted structures were maintained for 4 weeks without any disruption phenomenon (Fig. 10).

DISCUSSION

Immunosuppressive drugs must be administered after allogeneic or xenogeneic cell transplantation to prevent recipients' immune systems from rejecting the transplant. However, systemic administration of immunosuppressive drugs is usually associated with severe side effects. The developed CsA-loaded 3D drug carrier enables sustained release of CsA at a desired site and can therefore be emplaced near the transplanted tissue to deliver the drug only where it is needed, thereby avoiding the side effects. The drug carrier shows stable drug release kinetics over 4 weeks. This result indicates that a mechanically robust 3D drug carrier has great advantages for solving a number of problems, which have frequently occurred in hydrogel-based drug delivery systems. One of the main advantages of the developed drug carrier is the structural integrity of the drug-loaded hydrogel, which is a very important factor for the quantity and homogeneity of drug release (18) and for maintaining the optimal therapeutic drug levels by sustained drug release (13). In addition, we expected that the developed drug carrier has tailored properties to control the drug release behavior by modifying several parameters such as the size of the microspheres (5), the concentration of the hydrogel (51), and the ratio of lactide and glycolide of PLGA (51). The CsA-Algi gel can also be utilized as a carrier for cell transplantation. The CsA-loaded 3D drug carrier, which is composed of the CsA-Algi gel and the PCL/PLGA polymeric framework, can endure a compressive force up to several 10s of MPa (23,31,36,39,40,47), and can thus resist breaking and unintentional fast drug release. Many researchers have investigated the improvement of the mechanical properties of hydrogels. One of the best-known methods is an interpenetrating polymer network (IPN) system, which has garnered significant

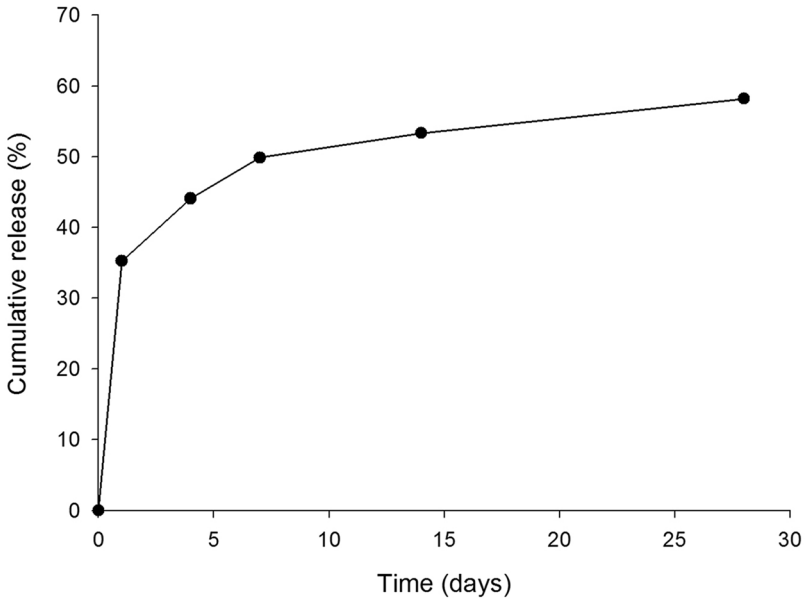

Figure 5. HPLC-based in vitro cumulative release profiles of CsA at 37°C from CsA-Algi gel as a function of time.

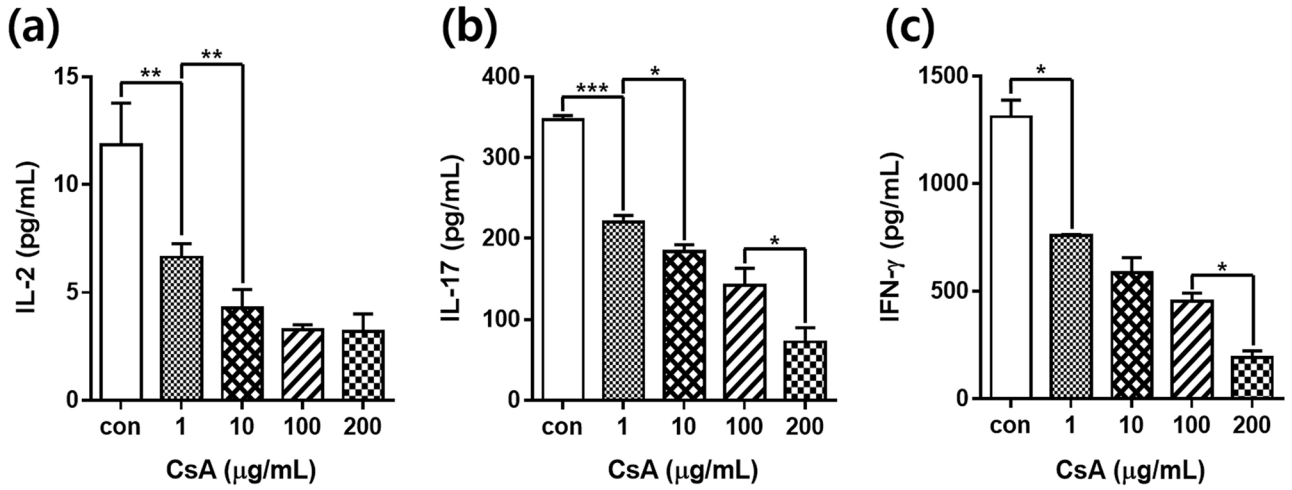

Figure 6. In vitro cytokine production versus concentration of CsA. ELISA of the production of (a) IL-2, (b) IL-17, (c) IFN-γ by ConA-activated spleen cells. *$p<0.05$, **$p<0.005$, ***$p<0.001$.

attention in the last two decades (30). Of all those systems, IPN-based double-network (DN) hydrogels have extremely high compressive fracture strength of around 17.2 MPa (15). In this respect, we have confirmed that the developed drug carrier has comparable mechanical stability with previously developed DN hydrogels (39). This mechanically stable structure might facilitate application to the high load-bearing tissue site for cell-based therapeutics, most representatively in orthopedics such as the regeneration of bone defects (24), the repair of joint surface damage (35), or the treatment of osteoarthritis (29).

The developed CsA-loaded 3D drug carriers are non-cytotoxic and show immunomodulatory effects in vitro. Adequate amounts of CsA were released from the carrier so that the released drug prohibited acceleration of secretion of cytokines (e.g., IL-2, IL-17, and IFN-γ) related to immune rejection. Th1 cytokines like IL-2 and IFN-γ secreted by Th1 cells are known to accelerate the cell-mediated immune response during the immune rejection process. Th17 cells selectively produce IL-17 cytokine and contribute to the acute rejection of xenotransplants (2,10,49). Consequently, the developed carrier can be applied to reduce acute transplant rejection by inhibition of cytokines from Th1 and Th17 cells, which are crucial factors of acute rejection in the xenogeneic cell transplantation.

The CsA-loaded 3D drug carrier has great potential to reduce immune rejection when used as a xenogeneic cell carrier in vivo. We delivered a human-derived cell source (HLF) to a subcutaneous site in a mouse. The CsA-loaded 3D drug carrier properly regulated mononuclear cell infiltration and T-cell-mediated rejection arising from xenogeneic cell transplantation. This result implies that the

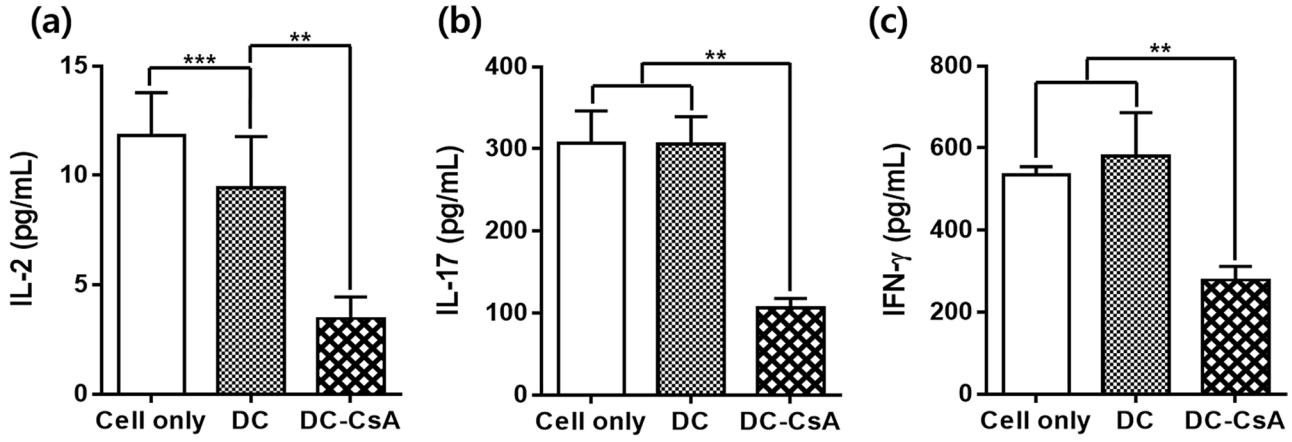

Figure 7. Quantification of immune rejection-related cytokines secreted by ConA-activated spleen cells on the CsA-loaded 3D drug carriers. ELISAs for the production of (a) IL-2, (b) IL-17, (c) IFN-γ (cell only, activated spleen cells; DC, 3D drug carriers without CsA; DC-CsA, CsA-loaded 3D drug carriers). **$p<0.005$, ***$p<0.001$.

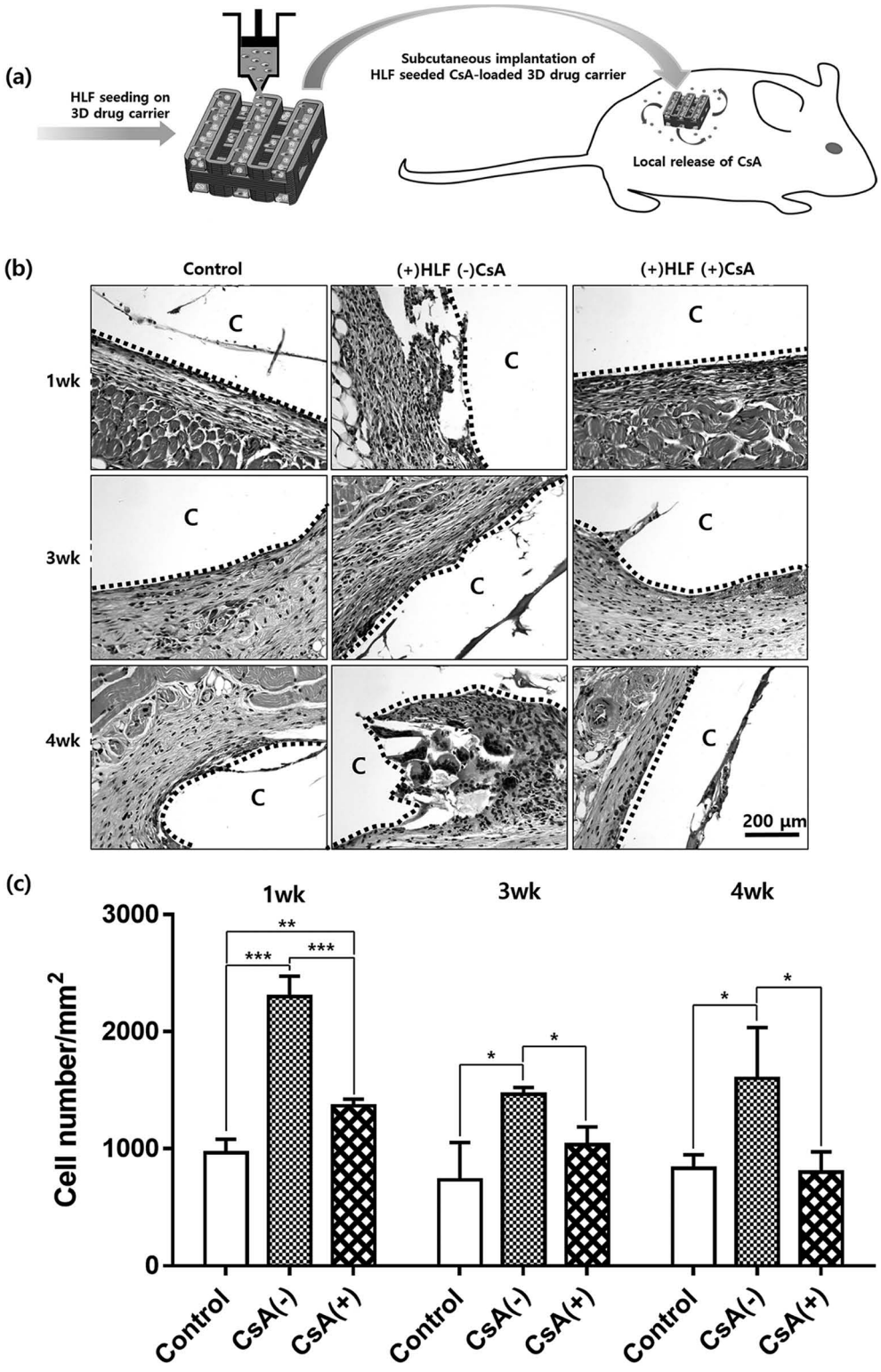

Figure 8. Subcutaneous implantation of HLF-seeded 3D drug carriers into BALB/c mouse. (a) Schematic design of HLF seeding and subcutaneous implantation of HLF-seeded 3D drug carriers into BALB/c mouse. (b) Visualized mononuclear cell infiltration by H&E [C, implanted 3D drug carrier; control, 3D drug carrier without CsA, (+)HLF (−)CsA, HLF seeded 3D drug carrier without CsA; (+)HLF (+)CsA, HLF seeded 3D drug carrier with CsA]. (c) The degree of the mononuclear cell infiltration [control, 3D drug carrier without CsA; CsA(−), HLF seeded 3D drug carrier without CsA, CsA(+), HLF seeded 3D drug carrier with CsA]. *$p<0.05$, **$p<0.005$, ***$p<0.001$.

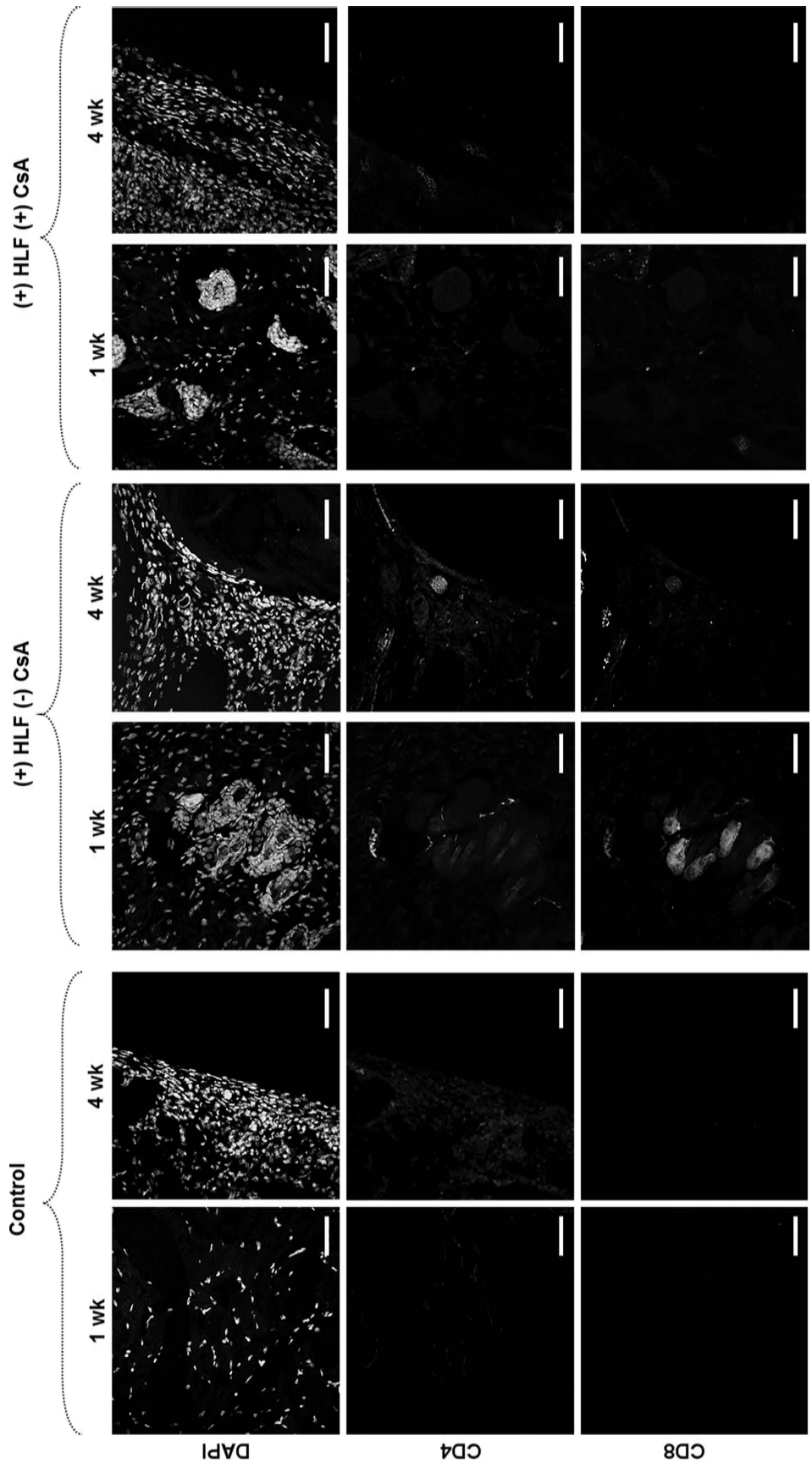

Figure 9. Immunofluorescence staining of T-cells surrounding the implants. Immunofluorescence staining of nuclei, $CD4^+$, and $CD8^+$ T cells at the surrounding tissues of the implanted 3D drug carriers.

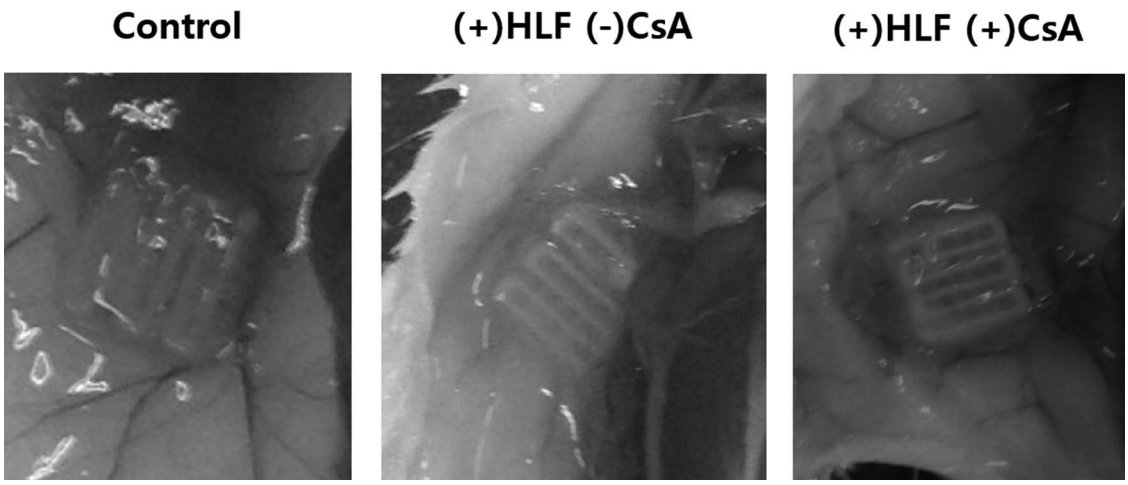

Figure 10. Shape of the implanted 3D drug carriers into BABL/c mouse model after 4 weeks [Control, 3D drug carrier without CsA; (+)HLF (−)CsA, HLF seeded 3D drug carrier without CsA; (+)HLF (+)CsA, HLF seeded 3D drug carrier with CsA].

immunosuppressive properties of CsA were conserved during the fabrication process and the release period, and that the locally delivered CsA can act as a calcineurin inhibitor to modulate immune rejection responses in vivo for up to 4 weeks. Many researchers have been trying to find a way to deliver CsA effectively, but most previous studies have been limited to systemic or transdermal/topical delivery; only one study has reported findings about local delivery of CsA by polymeric carrier systems such as electrospun nanofiber (19). In this respect, our developed CsA-loaded drug carrier suggests a possible method to obtain local and sustained CsA delivery.

Many reports have considered the limitations of microspheres or hydrogel-based drug delivery systems. In this study, several existing problems were overcome by combining microspheres and hydrogel. First, the CsA-Algi gel prevents phagocytosis of PLGA microspheres and retains microspheres at the injection site. Moreover, the reported drug/cell carrier has an advantage over hydrogel-based delivery systems due to its structural stability. Generally, the physiological conditions bring many problems regarding the breakup of the drug carriers (18). In this study, the load-bearing capacity of the developed CsA-loaded 3D drug carriers was improved, and the carriers maintained their shapes from 1 week to 4 weeks in vivo.

We have shown that the developed drug delivery system can act as CsA delivery carriers adequately. However, further investigation must be conducted to assess how the actual dose of the drug depends on the concentration of cells and to quantify the work efficiency of the delivered cells. Additionally, although we evaluated immunosuppressive effects over 4 weeks in vivo, the long-term effects of DC-CsA should be evaluated over the entire period of acute rejection.

This research could be a fundamental study for overcoming existing limitations, mainly caused by systemic immunosuppression. Especially, bio-3D printing technology should facilitate a wider range of applications, such as transplant surgery as well as cell-based therapy. For example, the drug carrier could be fabricated with the shape of membrane type, which might enable effective local immunosuppression to a specific area by easily sticking to the surgical site. Therefore, various practical research studies should also be performed in the future to achieve immunosuppression efficacy for actual applications such as the treatment of intractable diseases that require cell-based therapies or a type of transplantation.

CONCLUSION

We developed CsA-loaded 3D drug carriers for transplantation of xenogeneic cells. The developed carrier locally suppressed the immune response and therefore did not induce a rejection response after xenogeneic cell transplantation. The CsA-Algi gel prevents migration of microspheres; therefore, it cannot provoke an embolism; it can also prohibit phagocytosis by macrophages. Moreover, its improved load-bearing capacity enables the structure to maintain its original shape during the implantation period. The developed carrier is a promising solution to treat several diseases that require cell-based therapy, such as muscular dystrophy, degenerative disc disease, or myocardial infarction, and this system could be used as part of a cell therapy product to deliver cells and drugs efficiently to desired sites.

ACKNOWLEDGMENTS: This work was supported by the National Research Foundation of Korea (NRF) grant funded by the Korea Government (MSIP) (Nos. 2010-0018294 and 2011-0030075). The authors declare no conflicts of interest.

REFERENCES

1. Aksungur, P.; Demirbilek, M.; Denkbaş, E. B.; Vandervoort, J.; Ludwig, A.; Ünlü, N. Development and characterization of Cyclosporine A loaded nanoparticles for ocular drug delivery: Cellular toxicity, uptake, and kinetic studies. J. Control. Release 151(3):286–294; 2011.
2. Atalar, K.; Afzali, B.; Lord, G.; Lombardi, G. Relative roles of Th1 and Th17 effector cells in allograft rejection. Curr. Opin. Organ Transpl. 14(1):23–29; 2009.
3. Baran, D. A. Opinion: New directions in immunosuppression after heart transplantation. Nat. Rev. Cardiol. 10(7):422–427; 2013.
4. Bauer, D.; Wasmuth, S.; Hennig, M.; Baehler, H.; Steuhl, K.-P.; Heiligenhaus, A. Amniotic membrane transplantation induces apoptosis in T lymphocytes in murine corneas with experimental herpetic stromal keratitis. Invest. Ophthalmol. Vis. Sci. 50(7):3188–3198; 2009.
5. Berkland, C.; King, M.; Cox, A.; Kim, K. K.; Pack, D. W. Precise control of PLG microsphere size provides enhanced control of drug release rate. J. Control. Release 82(1): 137–147; 2002.
6. Bobadilla, N. A.; Gamba, G. New insights into the pathophysiology of cyclosporine nephrotoxicity: A role of aldosterone. Am. J. Physiol. 293(1):F2–F9; 2007.
7. Caicco, M. J.; Cooke, M. J.; Wang, Y. F.; Tuladhar, A.; Morshead, C. M.; Shoichet, M. S. A hydrogel composite system for sustained epi-cortical delivery of Cyclosporin A to the brain for treatment of stroke. J. Control. Release 166(3):197–202; 2013.
8. Chatterjee, A.; Bindu Sri, M.; Ashok, V. As a review on hydrogels as drug delivery in the pharmaceutical field. Int. J. Pharm. Chem. Sci. 1(2):20; 2012.
9. Daley, G. Q.; Scadden, D. T. Prospects for stem cell-based therapy. Cell 132(4):544–548; 2008.10.
10. Delios, M.; Josien, R.; Manghetti, M.; Amedei, A.; deCarli, M.; Cuturi, M. C.; Blancho, G.; Buzelin, F.; delPrete, G.; Soulillou, J. P. Predominant Th1 cell infiltration in acute rejection episodes of human kidney grafts. Kidney Int. 51(6):1876–1884; 1997.
11. Dimmeler, S.; Burchfield, J.; Zeiher, A. M. Cell-based therapy of myocardial infarction. Arterioscler. Thromb. Vasc. Biol. 28(2):208–216; 2008.
12. Farini, A.; Razini, P.; Erratico, S.; Torrente, Y.; Meregalli, M. Cell based therapy for Duchenne muscular dystrophy. J. Cell. Physiol. 221(3):526–534; 2009.
13. Gao, S. Q.; Maeda, T.; Okano, K.; Palczewski, K. A microparticle/hydrogel combination drug-delivery system for sustained release of retinoids. Invest. Ophthalmol. Vis. Sci. 53(10):6314–6323; 2012.
14. Gauthier, P.; Helderman, J. H. Cyclosporine avoidance. J. Am. Soc. Nephrol. 11(10):1933–1936; 2000.
15. Gong, J. P.; Katsuyama, Y.; Kurokawa, T.; Osada, Y. Double-network hydrogels with extremely high mechanical strength. Adv. Mater. 15(14):1155–1158; 2003.
16. Harris, R.; Lecumberri, E.; Heras, A. Chitosan-genipin microspheres for the controlled release of drugs: Clarithromycin, tramadol and heparin. Mar. Drugs 8(6):1750–1762; 2010.
17. He, Y.; Liu, Y. L.; Liu, Y.; Wang, J. C.; Zhang, X.; Lu, W. L.; Ma, Z. Z.; Zhu, X. A.; Zhang, Q. Cyclosporine-loaded microspheres for treatment of uveitis: In vitro characterization and in vivo pharmacokinetic study. Invest. Ophthalmol. Vis. Sci. 47(9):3983–3988; 2006.
18. Hoare, T. R.; Kohane, D. S. Hydrogels in drug delivery: Progress and challenges. Polymer 49(8):1993–2007; 2008.
19. Holan, V.; Chudickova, M.; Trosan, P.; Svobodova, E.; Krulova, M.; Kubinova, S.; Sykova, E.; Sirc, J.; Michalek, J.; Juklickova, M; Munzarova, M.; Zajicova, A. Cyclosporine A-loaded and stem cell-seeded electrospun nanofibers for cell-based therapy and local immunosuppression. J. Control Release 156(3):406–412; 2011.
20. Hong, J. C.; Kahan, B. D. Immunosuppressive agents in organ transplantation: Past, present, and future. Semin. Nephrol. 20(2):108–125; 2000.
21. Jain, S.; Mittal, A.; Jain, A. K.; Mahajan, R. R.; Singh, D. Cyclosporin A Loaded PLGA nanoparticle: Preparation, optimization, in-vitro characterization and stability studies. Curr. Nanosci. 6(4):422–431; 2010.
22. Joung, Y. K.; Choi, J. H.; Park, K. M.; Park, K. D. PLGA microparticle-embedded thermosensitive hydrogels for sustained release of hydrophobic drugs. Biomed. Mater. 2(4):269–273; 2007.
23. Kuo, C. K.; Ma, P. X. Ionically crosslinked alginate hydrogels as scaffolds for tissue engineering: Part 1. Structure, gelation rate and mechanical properties. Biomaterials 22(6):511–521; 2001.
24. Kwan, M. D.; Slater, B. J.; Wan, D. C.; Longaker, M. T. Cell-based therapies for skeletal regenerative medicine. Hum. Mol. Gen. 17(R1):R93–R98; 2008.
25. Lechler, R. I.; Sykes, M.; Thomson, A. W.; Turka, L. A. Organ transplantation - How much of the promise has been realized? Nat. Med. 11(6):605–613; 2005.26.
26. Lindvall, O.; Kokaia, Z.; Martinez-Serrano, A. Stem cell therapy for human neurodegenerative disorders–How to make it work. Nat. Med. 10:S42–S50; 2004.
27. Mascarell, L.; Auger, R.; Kanellopoulos, J. M.; Truffa-Bachi, P. The usage of alternative splice sites in Mus musculus synaptotagmin-like 2 gene is modulated by cyclosporin A and FK506 in T-lymphocytes. Mol. Immunol. 43(11): 1846–1854; 2006.
28. Matsuda, S.; Koyasu, S. Mechanisms of action of cyclosporine. Int. Immunopharmacol. 47(2–3):119–125; 2000.
29. Mobasheri, A.; Kalamegam, G.; Musumeci, G.; Batt, M. E. Chondrocyte and mesenchymal stem cell-based therapies for cartilage repair in osteoarthritis and related orthopaedic conditions. Maturitas 78(3):188–198; 2014.
30. Myung, D.; Waters, D.; Wiseman, M.; Duhamel, P. E.; Noolandi, J.; Ta, C. N.; Frank, C. W. Progress in the development of interpenetrating polymer network hydrogels. Polym. Adv. Tech. 19(6):647–657; 2008.
31. Naficy, S.; Kawakami, S.; Sadegholvaad, S.; Wakisaka, M.; Spinks, G. M. Mechanical properties of interpenetrating polymer network hydrogels based on hybrid ionically and covalently crosslinked networks. J. Appl. Polym. Sci. 130(4):2504–2513; 2013.
32. Nussenblatt, R. B.; Dinning, W. J.; Fujikawa, L. S.; Chan, C.-C.; Palestine, A. G. Local cyclosporine therapy for experimental autoimmune uveitis in rats. Arch. Ophthalmol. 103(10):1559; 1985.
33. Pei, C.; Xu, Y.; Jiang, J. X.; Cui, L.-J.; Li, L.; Qin, L. Application of sustained delivery microsphere of cyclosporine A for preventing posterior capsular opacification in rabbits. Int. J. Ophthalmol. 6(1):1; 2013.
34. Richer, S.; Judd, N.; Camp, S.; Doerschuk, C. Microsphere phagocytosis by alveolar macrophages in neonatal

mice and the role of TNF-alpha signaling. FASEB J. 15(4):A243–A243; 2001.
35. Roelofs, A.; Rocke, J.; De Bari, C. Cell-based approaches to joint surface repair: A research perspective. Osteoarthr. Cartil. 21(7):892–900; 2013.
36. Sa, M.-W.; Kim, J. Y. Effect of various blending ratios on the cell characteristics of PCL and PLGA scaffolds fabricated by polymer deposition system. Int. J. Precis. Eng. Man. 14(4):649–655; 2013.
37. Saralidze, K.; Koole, L. H.; Knetsch, M. L. W. Polymeric microspheres for medical applications. Materials 3(6): 3537–3564; 2010.
38. Seol, Y.-J.; Kang, T.-Y.; Cho, D.-W. Solid freeform fabrication technology applied to tissue engineering with various biomaterials. Soft Matter 8(6):1730–1735; 2012.
39. Shim, J. H.; Kim, J. Y.; Park, M.; Park, J.; Cho, D. W. Development of a hybrid scaffold with synthetic biomaterials and hydrogel using solid freeform fabrication technology. Biofabrication 3(3):034102; 2011.
40. Shim, J. H.; Lee, J. S.; Kim, J. Y.; Cho, D. W. Bioprinting of a mechanically enhanced three-dimensional dual cell-laden construct for osteochondral tissue engineering using a multi-head tissue/organ building system. J. Micromech. Microeng. 22(8):085014; 2012.
41. Shim, J.-H.; Moon, T.-S.; Yun, M.-J.; Jeon, Y.-C.; Jeong, C.-M.; Cho, D.-W.; Huh, J.-B. Stimulation of healing within a rabbit calvarial defect by a PCL/PLGA scaffold blended with TCP using solid freeform fabrication technology. J. Mater. Sci. Mater. Med. 23(12):2993–3002; 2012.
42. So, J. W.; Kim, S. H.; Baek, M. O.; Lim, J. Y.; Roh, H. W.; Lee, N. R.; Kim, M. S.; Ryu, G. H.; Cho, Y.-H.; Lee, S. J.; Min, B. H., Khang, G.; Le, H. B. Effect of size of PLGA microsphere on proliferation and phenotype for human intervertebral disc cells. Tissue Eng. Regen. Med. 4(4):577–582; 2007.
43. Tanabe, K. Calcineurin inhibitors in renal transplantation - What is the best option? Drugs 63(15):1535–1548; 2003.
44. Wang, X. Q.; Dai, J. D.; Chen, Z.; Zhang, T.; Xia, G. M.; Nagai, T.; Zhang, Q. Bioavailability and pharmacokinetics of cyclosporine A-loaded pH-sensitive nanoparticles for oral administration. J. Control. Release 97(3):421–429; 2004.
45. Wei, A.; Tao, H.; Chung, S. A.; Brisby, H.; Ma, D. D.; Diwan, A. D. The fate of transplanted xenogeneic bone marrow-derived stem cells in rat intervertebral discs. J. Orthop. Res. 27(3):374–379; 2009.
46. Wu, Y. J.; Yao, J.; Zhou, J. P.; Dahmani, F. Z. Enhanced and sustained topical ocular delivery of cyclosporine A in thermosensitive hyaluronic acid-based in situ forming microgels. Int. J. Nanomedicine 8:3587–3601; 2013.
47. Xu, T.; Binder, K. W.; Albanna, M. Z.; Dice, D.; Zhao, W.; Yoo, J. J.; Atala, A. Hybrid printing of mechanically and biologically improved constructs for cartilage tissue engineering applications. Biofabrication 5(1):015001; 2013.
48. Yang, Y.-G. Application of xenogeneic stem cells for induction of transplantation tolerance: Present state and future directions. Springer Semin. Immunopathol. 26:187–200; 2004.
49. Yu, X.; Jiang, Y. F.; Lu, L.; Gong, X.; Sun, X. G.; Xuan, Z. P.; Lu, L. J. A crucial role of IL-17 and IFN-gamma during acute rejection of peripheral nerve xenotransplantation in mice. Plos One 7(3):e34419; 2012.
50. Zhang, H.; Zhu, S.; Wang, W.; Wei, Y.; Hu, S. Transplantation of microencapsulated genetically modified xenogeneic cells augments angiogenesis and improves heart function. Gene Ther. 15(1):40–48; 2008.
51. Zheng, C.-H.; Gao, J.-Q.; Zhang, Y.-P.; Liang, W.-Q. A protein delivery system: Biodegradable alginate–chitosan–poly (lactic-co-glycolic acid) composite microspheres. Biochem. Biophys. Res. Commun. 323(4):1321–1327; 2004.